Predicting the Effect of Dissolved Carbon Dioxide on the Glass Transition Temperature of Poly(acrylic acid)

Gui-Ping Cao,[1] Tao Liu,[2] George W. Roberts[2]

[1]*State Key Laboratory of Chemical Engineering, East China University of Science and Technology, Shanghai 200237, China*
[2]*Department of Chemical and Biomolecular Engineering, North Carolina State University, Raleigh, North Carolina 27695-7905*

Received 15 January 2009; accepted 13 August 2009
DOI 10.1002/app.31278
Published online 7 October 2009 in Wiley InterScience (www.interscience.wiley.com).

ABSTRACT: The morphology and size of poly(acrylic acid) (PAA) particles produced by precipitation polymerization in supercritical CO_2 ($scCO_2$) depends on the glass transition temperature (T_g) of the polymer at reaction conditions. In this study, the use of the Sanchez–Lacombe equation of state (SL-EOS), in conjunction with Chow's equation, to predict the effect of CO_2 pressure on the T_g of PAA was evaluated. Characteristic parameters for PAA were determined by fitting density data. Characteristic parameters for CO_2 were determined by fitting density data in the supercritical region. When the SL-EOS was used in a purely predictive mode, with a binary interaction parameter (ψ) of 1, the solubility of CO_2 in PAA was underestimated and T_g was overestimated, although the trend of T_g with CO_2 pressure was captured. When was determined by fitting the SL-EOS to the measured sorption of $scCO_2$ in PAA, the calculated T_g's agreed very well with measured values.
 J Appl Polym Sci 115: 2136–2143, 2010

Key words: carbon dioxide; poly(acrylic acid); Sanchez–Lacombe; glass transition; binary interaction parameter; Chow's equation

INTRODUCTION

Carbon dioxide, especially supercritical CO_2 ($scCO_2$), has been evaluated as an alternative to many organic chemicals that are used in the synthesis and processing of polymers. The low cost, tunable properties, and environmentally benign nature of $scCO_2$ have led to its use as a medium for polymer synthesis, polymer precipitation by expansion from supercritical solutions, polymerization reactions within CO_2-swollen polymers, separations and fractionations, impregnation of solutes into polymer matrices, particle formation, foaming, and polymer blending.

It is well established that high-pressure CO_2 can plasticize amorphous and semicrystalline polymers, and consequently depress the glass transition temperature, T_g, dramatically.[1–8] The reduction of T_g is due primarily to intermolecular interactions between CO_2 and the polymer. An interesting example of this effect was recently reported by Liu et al.[9–12] in a study of the precipitation polymerization of acrylic acid in $scCO_2$ to form poly(acrylic acid) (PAA). Three different types of polymer morphology and different particle sizes, were obtained, depending on whether the reaction temperature was below, close to, or above the glass transition temperature of the CO_2-PAA mixture. Particle size is a critical factor in many commercial applications of PAA, which include dispersants, thickeners, flocculants, and superabsorbent polymers. The authors[9] suggested that polymer morphology and particle size might be controlled through manipulation of the polymerization conditions, so as to adjust the relationship between T_g and the polymerization conditions.

Liu et al.[9] measured the T_g of PAA as a function of CO_2 pressure. They showed that their data was well described by Chow's equation,[13] provided that experimental data for the solubility of CO_2 in PAA at the conditions of the T_g measurement was substituted directly into that equation. This analysis provided valuable guidance in understanding the polymerization behavior, and its relation to particle size and morphology. However, this approach is not predictive because of the need for experimental data on the solubility of CO_2 in PAA at temperatures and pressures close to those of the polymerization experiments.

Correspondence to: G.-P. Cao (gpcao@ecust.edu.cn) or G. W. Roberts (groberts@eos.ncsu.edu).
Contract grant sponsor: National Natural Science Foundation of China; contract grant numbers: 20490200, 20676031, 20876051.
Contract grant sponsor: STC Program of the National Science Foundation, USA; contract grant number: CHE-9876674.

This article explores the prediction of the solubility of CO_2 in PAA at supercritical conditions using the Sanchez–Lacombe equation of state (SL-EOS), and then using these calculated solubility to predict the effect of CO_2 pressure on the T_g of the PAA/CO_2 mixture, which have not been previously reported.

A BRIEF DESCRIPTION OF THE CALCULATION PROCEDURE

The review by Kirby and McHugh[14] provides a comprehensive discussion of the thermodynamic behavior of polymer-CO_2 systems. The SL-EOS is probably the most widely used model to describe CO_2 solubility in various polymer systems.[15–24] The SL-EOS is given by

$$\tilde{\rho}^2 + \tilde{P} + \tilde{T}\left(\ln(1-\tilde{\rho}) + \left(1 - \frac{1}{r}\right)\tilde{\rho}\right) = 0 \qquad (1)$$

In eq. (1), reduced $\tilde{T}$, $\tilde{P}$, and $\tilde{\rho}$ are defined as $\tilde{T} \equiv T/T^*$, $\tilde{P} \equiv P/P^*$, and $\tilde{\rho} \equiv \rho/\rho^*$. The number of lattice sites, r, occupied by a molecule, is related to the other three parameters and the molecular weight M of the pure component by $r = MP^*/RT^*\rho^*$.[25] For polymers, $r \to \infty$, and $1/r \to 0$. These parameters may be determined from pure-component experimental PVT data.[20] Characteristic parameters for CO_2 have been determined by a number of investigators.[19,20,22,23]

The characteristic parameters for a mixture can be calculated from those for the pure components as follows.

$$1/r_m = \phi_1/r_1 + \phi_2/r_2 = \phi_1/r_1 \qquad (2)$$

$$P^*_m = \phi_1 P^*_1 + \phi_2 P^*_2 - \phi_1\phi_2\Delta P^*_m \qquad (3)$$

$$\Delta P^*_m = P^*_1 + P^*_2 - 2P^*_{12} \qquad (4)$$

$$P^*_{12} = \psi\sqrt{P^*_1 P^*_2} \qquad (5)$$

$$T^*_m = \frac{P^*_m}{\frac{\phi_1 P^*_1}{T^*_1} + \frac{\phi_2 P^*_2}{T^*_2}} \qquad (6)$$

In eq. (2), ϕ_1 is the close-packed volume fraction of penetrant in the mixture and ϕ_2 the polymer. In eq. (5), ψ is the binary interaction parameter, which is a measure of the deviation of the mixture characteristic pressure from the geometric mean of the pure-component characteristic pressures. The SL-EOS is predictive only if ψ is known or can be accurately predicted *a priori*. However, there is no accepted means to make predictions of ψ. The binary interaction parameter is commonly assumed to be unity when components are nonpolar.[19] However, this is not the case for CO_2-PAA.

To determine the amount of penetrant sorbed into the polymer, the chemical potential of the penetrant in the pure phase is set equal to the chemical potential of the penetrant in the penetrant-polymer mixture.

$$\mu_{1,p} = \mu_{1,m} \qquad (7)$$

This equality is based on the assumption that there is no polymer in the fluid phase. This assumption is generally valid for CO_2, except for certain fluoropolymers and silane polymers. The chemical potential of penetrant in the pure phase is

$$\mu_{1,p} = RTr_1\left(-\frac{\tilde{\rho}_1}{\tilde{T}_1} + \frac{\tilde{P}_1}{\tilde{T}_1\tilde{\rho}_1} + \frac{(1-\tilde{\rho}_1)\ln(1-\tilde{\rho}_1)}{\tilde{\rho}_1} + \frac{\ln\tilde{\rho}_1}{r_1}\right) \qquad (8)$$

and that in the penetrant-polymer mixture is

$$\mu_{1,m} = RT\left(\ln\phi_1 + \phi_2 + \tilde{\rho}_m(M_1/\rho^*_1)\chi\phi_2^2 + r_1\left[-\frac{\tilde{\rho}_m}{\tilde{T}_1} + \frac{\tilde{P}_1}{\tilde{T}_1\tilde{\rho}_m} + \frac{(1-\tilde{\rho}_m)\ln(1-\tilde{\rho}_m)}{\tilde{\rho}_m} + \frac{\ln\tilde{\rho}_m}{r_1}\right]\right) \qquad (9)$$

The parameter χ is defined as $\chi = \Delta P^*_m/RT$. The weight fraction of penetrant (ω_1) has the following relationship with ϕ_1 and ϕ_2

$$\omega_1 = \phi_1/(\phi_1 + \phi_2(\rho^*_2/\rho^*_1)) \qquad (10)$$

If experimental solubility data are available, and if the characteristic parameters of the penetrant and polymer are specified, the binary interaction parameter ψ can be determined.

RESULTS AND DISCUSSION

Determination of characteristic parameters for CO_2

Kiszka et al.[21] have suggested that the characteristic parameters for a fluid be determined by fitting PVT data in the pressure and temperature range, where predictions are desired. Table I is a brief summary of previously determined characteristic parameters for CO_2, along with the ranges of temperature and pressure covered by the data from which these parameters were determined.

The values of the parameters in Table I are quite different, possibly because of the different regions of temperature and pressure that were covered, and possibly because of different strategies for calculating the parameters from experimental data.

In this study of the CO_2/PAA equilibrium, the temperature range of interest is 318–368 K and the pressure range is 13–29 MPa.[9] This region extends

TABLE I
Literature Values of the Characteristic Parameters for CO_2

Reference	T_1^*(K)	P_1^* (MPa)	ρ_1^* (g/L)	r_1	T (K)	P (MPa)
19	316	418.1	1369	5.11	308.15	0.5–7
20	283	659.6	1620	7.6	298.15	0.1–7
21	305	574.5	1510	6.60	308.15–341.15	0.1–25
22	280	719.5	1618	8.40	216.55–304.15	0.05–7.3

well beyond those covered by the studies in Table I. Therefore, a re-evaluation of the characteristic parameters for CO_2 was necessary.

The characteristic parameters of CO_2 were obtained in this research by fitting the SL–EOS to PVT data for CO_2 in the range of T from 318 to 368 K, and in the range of P from 13 to 29 MPa. The values of the characteristic parameters, P_1^*, ρ_1^*, and r_1, determined are shown in Table II. The experimental data was obtained from NIST.[26]

Figure 1 shows a comparison of the calculated and experimental PVT data for CO_2 in the range of temperature over which data was fitted. Visually, the experimental data agree well with the calculated values.

This value, a measure of the agreement between the NIST data and the density predicted by the SL-EOS with the parameters given in Table II, is quite small compared with the actual densities of CO_2 in the experimental region of this study.

To check whether the characteristic parameters in Table II can be used over a wider range of temperature and pressure, the density of CO_2 was calculated using these parameters, over a range of temperature from 323 to 393 K, and a pressure range from 0.345 to 34.45 MPa. Figure 2 is a comparison of the NIST data with calculations using the SL-EOS with the characteristic parameters given in Table II. The calculated densities over the wider range of conditions agree well with the NIST data. The most significant deviations occur at lower temperatures and pressures, where the density changes rapidly with both parameters.

Evaluation of characteristic parameters for PAA

Characteristic parameters for PAA have not been reported previously. The parameters used in this article should be determined by fitting the SL-EOS to experimental data for PAA. Because of the plasticization of $scCO_2$, PAA will be in rubber state when PAA is immersed in $scCO_2$. The experimental PVT data above the glass transition temperature will be used. Zoller and Walsh[27] have reported experimental PVT data for PAA in the temperature range from 296.55 to 497.45 K and in the pressure range from 0 to 200 MPa for intervals of 20MPa. However, the most relevant pressure range for our present study is 6.5–28 MPa. If all of Zoller and Walsh's original PVT data of PAA were used directly to find the parameters of S-L EOS, the calculated PVT data gave a very poor fitting to the experimental data, just because the range of pressure was greatly wider than that in our study. Therefore, the Tait equation[28,29] was fit to the data, and was used to interpolate with respect to temperature and pressure.

TABLE II
Characteristic Parameters for CO_2 obtained by Nonlinear Regression of NIST[26] Data (P = 13–28 MPa; T = 318–368 K)

T_1^* (K)	P_1^* (MPa)	ρ_1^* (g/L)	r_1
327	453.5	1460	5.19

Different forms of the Tait equation have been used to represent the PVT behavior for a number of liquids, including polymeric liquids.[28,30–32] The equation used here is:

$$\frac{\rho_0}{\rho} = 1 - c\ln\left\{1 + \frac{P}{b_1\exp(-b_2T)}\right\} \qquad (11)$$

In eq. (11), ρ is the density at pressure P and temperature T; ρ_0 is the density at $P = 1$ bar and the same temperature (T); and c, b_1, and b_2 are constants.

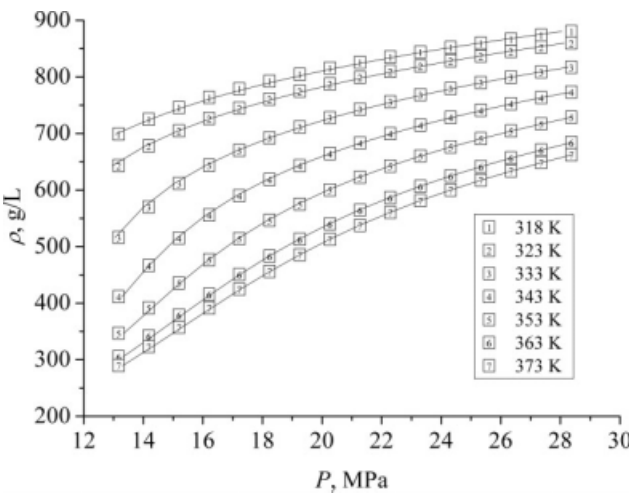

Figure 1 Density of CO_2 versus CO_2 pressure at different temperatures. (Symbols: density values from NIST.[26] Lines: densities calculated from the SL-EOS using the characteristic parameters in Table II).

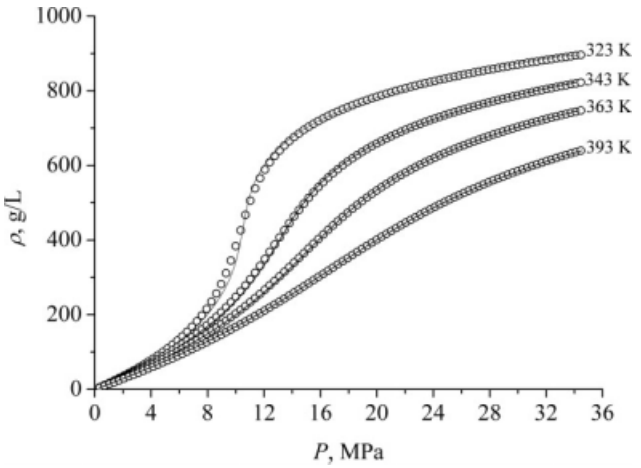

Figure 2 Density of CO_2 versus pressure over a wider range of temperature and pressure. (Symbols: density values from NIST.[26] Lines: densities calculated from the SL-EOS using the characteristic parameters in Table II).

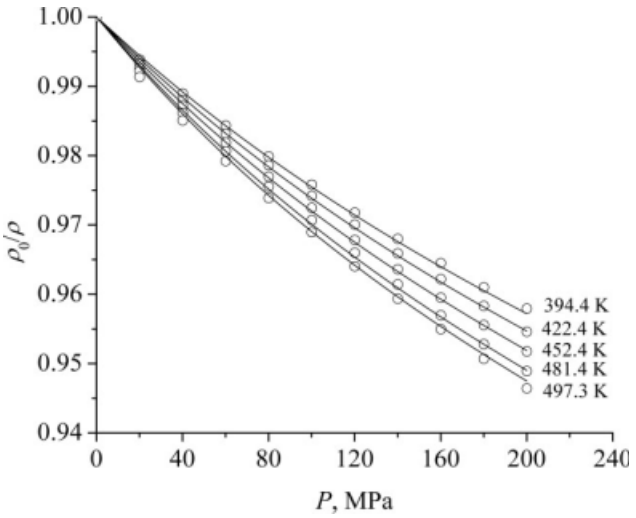

Figure 3 Fit of the Tait equation to density data for PAA above T_g. (Lines: densities calculated from the Tait equation [eq. (15)] using the parameters in Table III. Circles: densities from Ref. 27).

These constants were determined for PAA in the region above T_g by nonlinear regression of the data of Zoller and Walsh. The resulting values are shown in Table III.

Figure 3 shows the fit of the Tait equation to the experimental data for PAA above T_g. The PAA densities calculated from the Tait equation fit the experimental data reasonably well, although ρ_0/ρ is slightly overpredicted at high temperatures and low pressures.

The "data" that are required to determine the characteristic parameters for PAA in the pressure range from 6.5 to 30.0 MPa were calculated from eq. (11). Then, the characteristic parameters in the SL-EOS were obtained by nonlinear regression. Table IV gives the final values of the characteristic parameters for pure PAA above T_g.

Figure 4 shows a comparison of the PAA densities calculated from the SL-EOS using these parameters with the "experimental" data from the Tait equation. The densities calculated from the SL-EOS match the "experimental" data quite well. In subsequent calculations, the values of T_2^*, P_2^*, and ρ_2^* shown in Table IV have been used.

Solubility of CO_2 in PAA at supercritical conditions

Liu et al.[9] measured the solubility of CO_2 in PAA at temperatures between 318 and 368 K and at pressures between about 6 and 28 MPa. Table V shows a comparison between the measured solubility and that calculated from the SL-EOS using the characteristic parameters for CO_2 and PAA that are shown earlier, and using $\psi = 1.0$. The predicted solubility of CO_2 in PAA is consistently lower than the measured solubility by roughly 30%.

Condo et al.[33] have shown that the binary interaction parameter has a major influence on the solubility of the penetrant in the polymer, and consequently, on the variation of T_g with penetrant pressure.

A value of ψ for CO_2-PAA mixtures was obtained by fitting experimental data for the solubility of CO_2 in PAA. The experimental solubility data for CO_2 in PAA were obtained from Liu et al.[9] Twenty data points were available. The optimal value of the binary interaction parameter, ψ, was determined to be 1.03.

Table V shows the measured solubility of CO_2 in PAA, ϕ_{1exp}, plus the solubility calculated from the SL-EOS, ϕ_{1mod}, using $\psi = 1.03$. As noted previously, the calculated solubility for $\psi = 1.0$ consistently underpredict the measured solubility. The solubility data calculated with $\psi = 1.03$ are much closer to the measured solubility. The standard deviation is 0.0049.

TABLE III
Parameters for PAA in the Tait Equation ($T > T_g$)

T (°C)	P (MPa)	c ($\times 10^2$)	b_1 ($\times 10^{-3}$) (bars)	b_2 ($\times 10^3$) (K^{-1})
24.3–224.3	0–200	7.1138	7.1132	2.7284

TABLE IV
Characteristic Parameters in the SL-EOS for Pure PAA Above T_g

T_2^* (K)	P_2^* (atm)	ρ_2^* (g/L)
859	937.3	1483

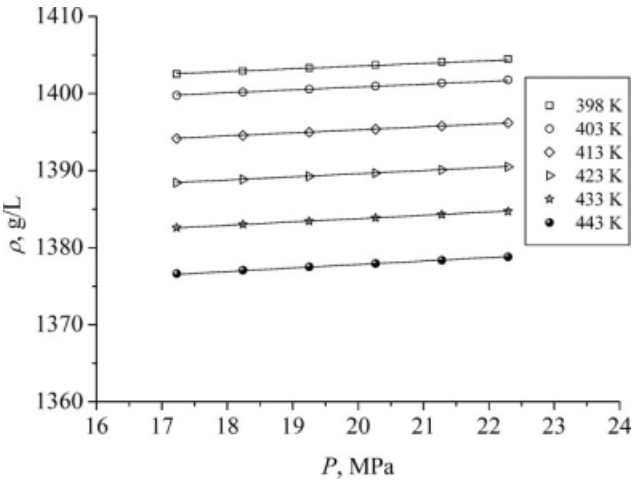

Figure 4 Comparison of calculated PAA density with the "experimental" PAA density. (Symbols: "experimental" density from the Tait equation. Lines: calculated density from SL-EOS using the characteristic parameters in Table IV).

Figure 5 is a visual comparison of the experimental and calculated solubility of CO_2 in PAA, using $\psi = 1.03$, over the temperature range from 318 and 368 K and the pressure range from 6 to 28 MPa. In Figure 5, the temperature values are lower than the T_g of pure PAA, 394.05 K,[9] at standard pressure (1 atm). The solubility of CO_2 in PAA was calculated using the characteristic parameters of PAA in Table IV, in which the temperature was higher than 394.05 K. It is seemingly contradictive for the two different ranges of temperature. Nevertheless, the plasticization of PAA by $scCO_2$ results in the depression of T_g, and makes PAA in or near rubber state over the range of temperature shown in Figure 5. As stated earlier, the calculated and experimental solubility agree reasonably well, although the fit of the SL-EOS to the data is not perfect, especially at the lower temperatures, which is probably resulted from that PAA is close to glass region, and slightly far from rubber region. However, the ability of the SL-EOS to describe the data is improved significantly by the use of an accurate value of ψ.

The glass transition temperature

The effect of a dissolved component on the T_g of a polymer can be estimated using Chow's equation.[13,34,35]

$$\ln\left(\frac{T_{g,\mathrm{mix}}}{T_{g,0}}\right) = \beta[\theta \ln \theta + (1-\theta)\ln(1-\theta)] \qquad (12)$$

where

$$\theta = \frac{M_u}{zM_d}\frac{\omega_1}{1-\omega_1} \qquad (13)$$

$$\beta = \frac{zR}{M_u \Delta C_{\mathrm{pp}}} \qquad (14)$$

In eqs. (12)–(14), $T_{g,\mathrm{mix}}$ is the glass-transition temperature of the polymer containing a weight fraction, ω_1, of the dissolved component; $T_{g,0}$ is the glass-transition temperature of the pure polymer; M_u is the

TABLE V
Measured and Calculated Values of CO_2 Solubility in PAA

No.	T (°C)	P (MPa)	$\phi_{1\mathrm{exp}}$[9]	$\phi_{1\mathrm{mod}}$ ($\psi = 1.03$)	$\phi_{1\mathrm{mod}}$ ($\psi = 1.0$)
1	323.15	6.89	0.0645	0.0699	0.0441
2	323.15	13.79	0.1021	0.0988	0.0612
3	323.15	20.68	0.1113	0.1086	0.0668
4	323.15	27.57	0.1179	0.1169	0.0715
5	333.15	6.89	0.0542	0.0609	0.0392
6	333.15	13.79	0.0869	0.0927	0.0586
7	333.15	20.68	0.0992	0.1039	0.0652
8	333.15	27.57	0.1052	0.1127	0.0703
9	343.15	6.89	0.0485	0.0538	0.0353
10	343.15	13.79	0.0788	0.0860	0.0554
11	343.15	20.68	0.0949	0.0990	0.0633
12	343.15	27.57	0.1028	0.1084	0.0689
13	353.15	6.89	0.0452	0.0480	0.0320
14	353.15	13.79	0.0717	0.0793	0.0520
15	353.15	20.68	0.0910	0.0941	0.0612
16	353.15	27.57	0.1002	0.1043	0.0674
17	363.15	6.89	0.0410	0.0432	0.0292
18	363.15	13.79	0.0673	0.0730	0.0486
19	363.15	20.68	0.0896	0.0892	0.0590
20	363.15	27.57	0.1005	0.1001	0.0658

Calculated values are from the S-L EOS with binary interaction parameters (ψ) of 1.0 and 1.03.

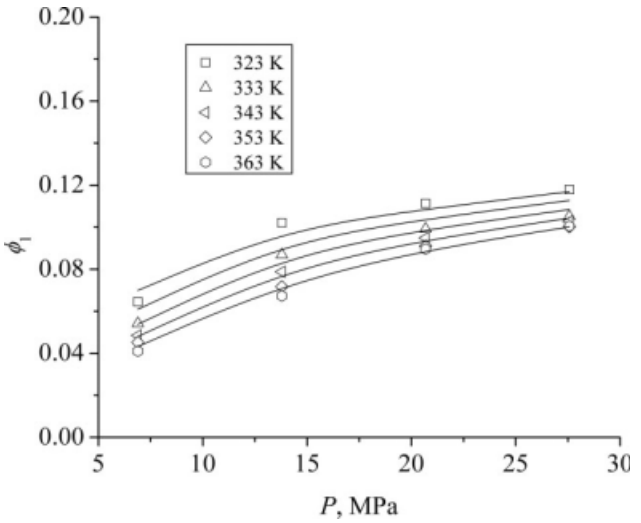

Figure 5 Experimental and calculated solubility of CO_2 in PAA. (Points are experimental data[9]; lines are calculations using the SL-EOS with $\psi = 1.03$).

molar mass of the polymer repeat unit; M_d is the molar mass of the dissolved component; R is the gas constant; ΔC_{pp} is the excess transition isobaric specific heat of the pure polymer, and z is the lattice coordination number, which can be either 1 or 2. For polymers with small repeat units, such as polystyrene and poly(methyl methacrylate), $z = 1$ gives the best fit of the experimental results. For polymers with larger repeat units, such as polycarbonate and poly(ethylene terephthalate), $z = 2$ usually gives a better description of the data.[5,7,36–38] Liu et al.[9] reported that Chow's equation agreed well with the experimental data for PAA when: $z = 1$; $T_{g,0} = 394.05$ K; and $\Delta C_{pp} = 0.4$ J/(g K). To use Chow's equation in a completely predictive mode, it must be possible to predict the solubility of the dissolved component, ω_1. Liu et al. used experimental solubility data to calculate ω_1 from eq. (10), and subsequently to calculate T_g. This validated Chow's equation for the PAA/CO_2 system, but did not establish a predictive approach.

The glass-transition temperature of the CO_2-PAA mixture can be predicted using eq. (12). The results are shown in Figure 6. The calculations were performed by choosing a temperature and CO_2 pressure, calculating ϕ_1 at these conditions, as described in the previous section, and then calculating ω_1 from eq. (10). If the calculated T_g did not match the starting temperature, the calculation was repeated until the calculated T_g matched the starting temperature. Calculations were performed for $\psi = 1.0$ and $\psi = 1.03$, respectively. As the CO_2 pressure is increased, the predicted value of T_g decreases. The predicted values of T_g for $\psi = 1.03$ match the experimental data quite well, despite the deviations in φ_1 shown in Table V. For $\psi = 1.0$, the predicted values of T_g are consistently high, with the largest deviations at the highest pressures. This is because the SL-EOS with $\psi = 1.0$ consistently underpredicts the solubility of CO_2 in PAA, as shown in Table V. Nevertheless, this case captures the trend of the data, and may provide a reasonable first approximation to the actual behavior.

A different presentation of the effect of CO_2 pressure on the glass-transition temperature is shown in Figure 7. The lines labeled with temperatures are the

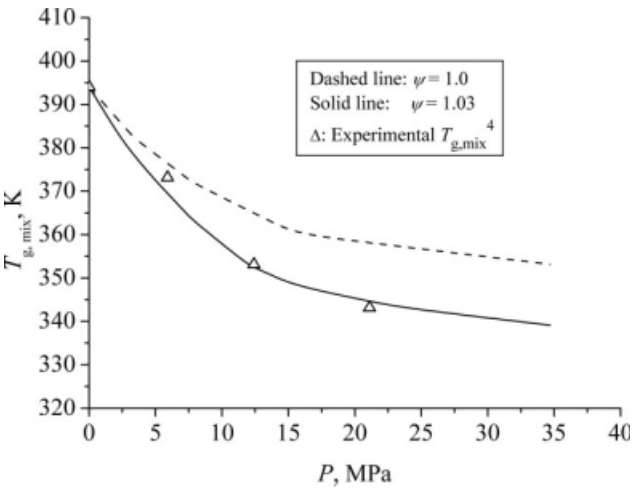

Figure 6 Comparison of experimental and calculated glass-transition temperatures for binary interaction parameters of $\psi = 1.0$ and $\psi = 1.03$.

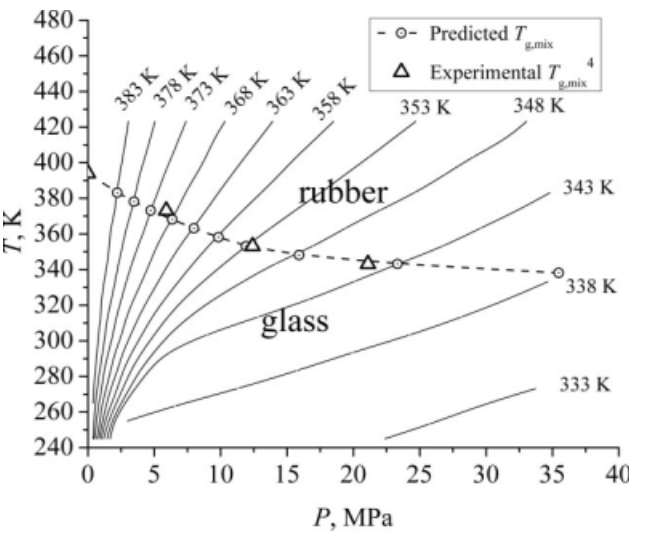

Figure 7 Glass transition temperature isopleths. (The solid lines are the $T_{g,mix}$ isopleths of the CO_2-PAA mixture. The dashed line with hollow round points is the locus of predicted $T_{g,mix}$ values with a $T_{g,0}$ of pure PAA = 394.05 K. The triangular points are the experimental $T_{g,mix}$ values from Ref. [9]. The binary interaction parameter is 1.03).

isopleths of $T_{g,\mathrm{mix}}$. On one of these lines, the solubility, ϕ_1, and therefore the glass transition temperature, $T_{g,\mathrm{mix}}$, are constant, i.e., at any point on an isopleth, the temperature and pressure are such that the CO_2 solubility remains unchanged.

The circular symbols on the isopleths mark the points where the temperature and T_g, as calculated from eq. (12) using $\psi = 1.03$, are equal. These points define the boundary between the rubbery and glassy regions, as noted in Figure 7. Experimental values of $T_{g,\mathrm{mix}}$[9] also are shown in the figure. As noted previously, the experimental data agree well with the predicted values.

Some of the temperatures used to make the calculations shown in Figure 7 are below the glass-transition temperature of the polymer. The polymer is glassy at these conditions. When $T < T_g$, the calculations of both ω_1 and T_g are approximate, since the characteristic parameters for PAA were derived from data in the rubbery region. Nevertheless, Figure 7 will be very useful to predict the morphology and particle sizes of the produced PAA in appropriate conditions, and design the experiments to control the morphology and particle sizes.

Condo et al.[33] and Kikic et al.[39] defined four types of glass-transition behavior for CO_2-polymer mixtures, depending on the value of the binary interaction parameter, ψ. With increasing ψ, the glass-transition behavior type changes from Type I through Types II and III to Type IV. With Type I behavior, there is a minimum in the T_g versus pressure curve. Therefore, under certain conditions, two glass transitions might be observed as the pressure is reduced at constant temperature. This behavior is relevant to the PAA/CO_2 system, since T_g was measured by decreasing the pressure isothermally.[9] Note also that Chow's equation predicts that T_g will go through a minimum at $\theta = 0.50$, which corresponds to $\omega = 0.23$ for PAA. Concerning the minimum T_g value of PAA, it can be explained as that the pressure has two roles on the PAA. One is high pressure promotes CO_2 dissolving in PAA and causes the depression of T_g. On the other hand, high pressure has a static hydraulic role on PAA, making PAA compressed and leading the increasing of T_g.

CONCLUSIONS

The Sanchez–Lacombe equation of state (SL-EOS) was demonstrated to be a sound thermodynamic model for describing the CO_2-PAA system at supercritical conditions. The characteristic parameters of CO_2 in the SL-EOS were determined over a wide range of temperature and pressure in the supercritical region by fitting density data from NIST. The characteristic parameters for "rubbery" PAA were determined over a wide range of pressure by fitting previously measured densities. A binary interaction parameter in the SL-EOS was determined by fitting data for the sorption of CO_2 in PAA. The CO_2 solubility in PAA is very sensitive to the value of the binary interaction parameter.

The resulting model permitted the major thermodynamic properties of CO_2-PAA mixtures, namely the CO_2 solubility, to be predicted. Chow's equation then could be used to predict the dependence of the glass-transition temperature of PAA on the CO_2 pressure. These predictions agreed very well with measured values of T_g, provided that an experimentally determined value of the binary interaction parameter was used in the SL-EOS. Moreover, the glass-transition temperature is predicted to exhibit Type I behavior. For the completely predictive case of $\psi = 1.0$, the predicted T_g values were higher than the measured values.

The authors thank Professor Ruben G. Carbonell for helpful comments and suggestions.

NOMENCLATURE

b_1, b_2, c	constants in Tait's equation
ΔC_{pp}	excess transition isobaric specific heat of the pure polymer, J/(g.K)
M	molecular weight, g/mol
M_d	molar mass of the dissoved component in the polymer, g/mol
M_u	molar mass of the repeat unit in the polymer, g/mol
N_M	total number of data points
P	pressure, MPa
$\tilde{P}$	reduced pressure
P^*	characteristic pressure, MPa
P^*_m	characteristic pressure for the mixture, MPa
R	gas constant, 8.314 J/(mol.K)
s	objective function
T	temperature, K
$\tilde{T}$	reduced temperature
T^*	characteristic temperature, K
T^*_m	characteristic temperature for the mixture, K
T_g	glass transition temperature, K
$T_{g,0}$	glass transition temperature at atmospheric pressure, K
$T_{g,\mathrm{mix}}$	glass transition temperature of the mixture, K
z	coordination number
β	constant in Chow's equation
ϕ	volumetric fraction of component in mixture
μ	chemical potential
θ	constant in Chow's equation

ρ	density, g/L
$\tilde{\rho}$	reduced density
ρ^*	characteristic density, g/L
ρ^*_m	characteristic density for the mixture, g/L
σ	standard deviation
ω	weight fraction of a component in mixture
ψ	binary interaction parameter

Subscription

1	Penetratant
2	Polymer
m	Mixture
p	Pure component

References

1. Zhang, Q.; Xanthos, M.; Dey, S. K. ASME Cell Microcell Mater 1998, 75.
2. O'Neill, M. L.; Handa, Y. P. ASTM STP V, Philadelphia, Pennsylvania (1249), 1994.
3. Kamiya, Y.; Mizoguchi, K.; Naito, Y. J Polym Sci Part B: Polym Phys 1990, 28, 1955.
4. Mi, Y.; Zheng, S. Polymer (Guildford) 1998, 39, 3709.
5. Handa, Y. P.; Lampron, S.; O'neill, M. L. J Polym Sci Part B: Polym Phys 1994, 32, 2549.
6. Zhang, Z.; Handa, Y. P. J Polym Sci Part B: Polym Phys 1998, 36, 977.
7. Chiou, J. S.; Barlow, J. W.; Paul, D. R. J Appl Polym Sci 1985, 30, 2633.
8. Edwards, R. R.; Tao, Y.; Xu, S.; Wells, P. S.; Yun, K. S.; Parcher, J. F. J Polym Sci Part B: Polym Phys 1998, 36, 2537.
9. Liu, T.; Garner, P.; Desimone, J. M.; Roberts, G. W.; Bothun, G. D. Macromolecules 2006, 39, 6489.
10. Liu, T.; Desimone, J. M.; Roberts, G. W. J Polym Sci Part A: Polym Chem 2005, 43, 2546.
11. Liu, T.; Desimone, J. M.; Roberts, G. W. Chem Eng Sci 2006, 61, 3129.
12. Liu, T.; Desimone, J. M.; Roberts, G. W. Polymer 2006, 47, 4276.
13. Chow, T. S. Macromolecules 1980, 13, 362.
14. Kirby, C. F.; Mchugh, M. A. Chem Rev 1999, 99, 565.
15. Liu, D. H.; Li, H. B.; Noon, M. S.; Tomasko, D. L. Macromolecules 2005, 38, 4416.
16. Pantoula, M.; Panayiotou, C. The J Supercrit Fluids 2006, 37, 254.
17. Voutsas, E. C.; Pappa, G. D.; Magoulas, K.; Tassios, D. P. Fluid Phase Equilib 2006, 240, 127.
18. Park, H.; Park, C. B.; Tzoganakis, C.; Tan, K. H.; Chen, P. Ind Eng Chem Res 2006, 45, 1650.
19. Hariharan, R.; Freeman, B. D.; Garbonell, R. G.; Sarti, G. C. J Appl Polym Sci 1993, 50, 1781.
20. Pope, D. S.; Sanchez, I. C.; Koros, W. J.; Fleming, G. K. Macromolecules 1991, 24, 1779.
21. Kiszka, M. B.; Meilchen, M. A.; Mchugh, M. A. J Appl Polym Sci 1988, 36, 583.
22. Kilpatrick, P. K.; Chang, S. H. Fluid Phase Equilib 1986, 30, 49.
23. Sanchez, I. C.; Lacombe, R. H. Theory J Phys Chem 1976, 80, 2352.
24. Sanchez, I. C.; Lacombe, R. H. J Polym Sci: Polym Lett Ed 1977, 15, 71.
25. Sanchez, I. C.; Lacombe, R. H. Macromolecules 1978, 11, 1145.
26. NIST. 2008.
27. Zoller, P.; Walsh, D. J.; Walsh, W. Standard Pressure-Volume-Temperature Data for Polymers; Technomic Publishing Company, Inc.: Lancaster, Pennsylvania, 1995.
28. Quach, A.; Simha, R. J Appl Phys 1971, 42, 4592.
29. Beret, S.; Prausnitz, J. M. Macromolecules 1975, 8, 536.
30. Benson, M. S.; Winnick, J. J Chem Eng Data 1971, 16, 154.
31. Eduljee, H. E.; Newitt, D. M.; Weale, K. E. J Chem Soc 1951, 683, 3086.
32. Maloney, D. P.; Prausnitz, J. M. J Appl Polym Sci 1974, 18, 2703.
33. Condo, P. D.; Sanchez, I. C.; Panayiotou, C. G.; Johnston, K. P. American Chemical Society, 1992; p 6119.
34. Lin, H.; Freeman, B. D.; Kalakkunnath, S.; Kalika, D. S. J Membr Sci 2007, 291, 131.
35. Nalawade, S. P.; Nieborg, V. H. J.; Picchioni, F.; Janssen, L. P. B. M. Powder Technol 2006, 170, 143.
36. Handa, Y. P.; Capowski, S.; O'neill, M. L. Thermochim Acta 1993, 226, 177.
37. Banerjee, T.; Lipscomb, G. C. J Appl Polym Sci 1998, 68, 1441.
38. Chiou, J. S.; Paul, D. R. J Appl Polym Sci 1986, 32, 2897.
39. Kikic, I.; Vecchione, F.; Alessi, P.; Cortesi, A.; Eva, F.; Elvassore, N. Ind Eng Chem Res 2003, 42, 3022.